Chronic Exposure to Carbon Nanotubes Induces Invasion of Human Mesothelial Cells through Matrix Metalloproteinase-2

Warangkana Lohcharoenkal,[†] Liying Wang,[⊥] Todd A. Stueckle,[⊥] Cerasela Zoica Dinu,[‡] Vincent Castranova,[⊥] Yuxin Liu,[§] and Yon Rojanasakul[†,*]

[†]Department of Pharmaceutical Sciences and Mary Babb Randolph Cancer Center, [‡]Department of Chemical Engineering, and [§]Department of Computer Science and Electrical Engineering, West Virginia University, Morgantown, West Virginia 26506, United States and [⊥]Pathology and Physiology Research Branch, National Institute for Occupational Safety and Health, Morgantown, West Virginia 26505, United States

ABSTRACT Malignant mesothelioma is one of the most aggressive forms of cancer known. Recent studies have shown that carbon nanotubes (CNTs) are biopersistent and induce mesothelioma in animals, but the underlying mechanisms are not known. Here, we investigate the effect of long-term exposure to high aspect ratio CNTs on the aggressive behaviors of human pleural mesothelial cells, the primary cellular target of human lung mesothelioma. We show that chronic exposure (4 months) to single- and multiwalled CNTs induced proliferation, migration, and invasion of the cells similar to that observed in asbestos-exposed cells. An up-regulation of several key genes known to be important in cell invasion, notably matrix metalloproteinase-2 (MMP-2), was observed in the exposed mesothelial cells as determined by real-time PCR. Western blot and enzyme activity assays confirmed the increased expression and activity of MMP-2. Whole genome microarray analysis further indicated the importance of MMP-2 in the invasion gene signaling network of the exposed cells. Knockdown of MMP-2 in CNT and asbestos-exposed cells by shRNA-mediated gene silencing effectively inhibited the aggressive phenotypes. This study demonstrates CNT-induced cell invasion and indicates the role of MMP-2 in the process.

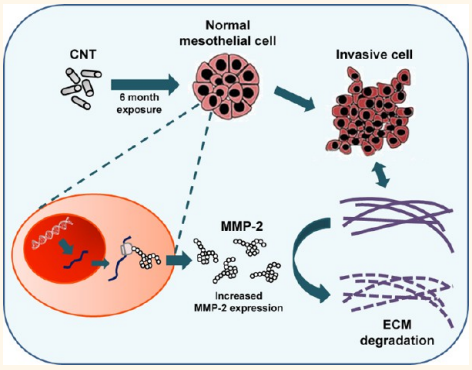

KEYWORDS: carbon nanotubes · asbestos · mesothelioma · MMP-2 · mesothelial cells · cell invasion

Carbon nanotubes (CNTs) are high aspect ratio nanoparticles (HARNs) comprising single or concentrically stacked multiwalled graphene sheets rolled into a cylinder. CNTs have been used in a wide range of applications, in fields as diverse as electronics and medicine.[1,2] Due to their widespread use and unknown health consequences, it is important to determine their safety especially in long-term occupational and environmental exposures. The high aspect ratio and mode of exposure of CNTs which is similar to asbestos fibers have raised a particular concern regarding the potential carcinogenicity of CNTs, especially in the pleural spaces which are key target tissues for asbestos-related diseases.[3]

It has been reported that after the inhalation of HARNs, they can migrate into the alveolar interstitial compartment of the lung. The low clearance rate from the interstitium would lead to biopersistence of CNTs in the lung. It has been demonstrated that 97, 38, and 16% of CNTs remained in the lung at 1, 3, and 6 months after a single intratracheal instillation.[4] Deposition of CNTs in the alveolar airspaces, penetration through the pleural interstitium to the parietal pleura, clearance failure due to length-restricted clearance through the normal stomatal clearance system, and the concomitant development of a pathogenic response in both subpleural and visceral pleura regions have previously been reported.[5] Numerous *in vivo* studies have already demonstrated that both single-walled (SW) and multiwalled (MW) CNTs, when instilled into the lungs of rodents, have the potential to cause

* Address correspondence to yrojan@hsc.wvu.edu.

Received for review May 3, 2013 and accepted August 7, 2013.

Published online August 08, 2013
10.1021/nn402241b

inflammation, fibrosis (scarring of the lungs), and granuloma (small nodule) formation,[6−8] consistent with the pathogenic behaviors of asbestos. Although differences in CNT length, diameter, dispersion, and functionalization impact fate, cellular uptake, persistence, and pathological responses in murine lung models, similar fiber dimensions (*i.e.*, high aspect ratio) and biopersistence compared to asbestos have long been recognized as important characteristics in CNT fiber pathogenicity.[9] The translocation of a fraction of all deposited particles and fibers to the pleural space can initiate mesothelial injury and inflammation that over time leads to pleural pathology, including mesothelioma.[10] The mechanism of production of pleural mesothelioma is not well understood, but the contact between fibers and mesothelial cells is a reasonable supposition.

Numerous studies have demonstrated effects such as genotoxicity and inflammation following the exposure of mesothelial cells to asbestos and other fibers *in vitro*.[11,12] Although several of the published studies investigated the acute *in vitro* effects of CNTs such as DNA breakage, alteration of cell proliferation, as well as cell activation *via* AP-1, NF-κB, and AKT in both normal and malignant mesothelial cells,[13−15] the effects of chronic exposure to CNTs on human mesothelial cells have not been reported. Since mesothelioma pathogenesis is a long-term multistep process, we chronically exposed human pleural mesothelial MeT5A cells to low-dose noncytotoxic concentrations of SWCNTs, MWCNTs, and asbestos in culture over a 4 month period. The cells were then evaluated for their proliferative, migratory, and invasive properties to study the long-term cellular effects of CNTs.

Cell migration is defined as the movement of individual cells or a group of cells from one location to another. It is central to many physiological and pathological processes including wound healing, cancer, and inflammation.[16] Cell invasion refers to three-dimensional migration of cells as they penetrate an extracellular matrix (ECM) and is a process typically associated with cancer cell metastasis.[17] Cell migration and invasion are multistep processes facilitated by a variety of factors including integrin signaling, focal-contact formation, and actomyosin-dependent contractility. ECM-degrading enzymes such as matrix metalloproteinases (MMPs), urokinase plasminogen activator (uPA), and cathepsins are frequent crucial factors underlying the process of cell invasion through the surrounding tissue.[18] Our study focused on comparing the effect of chronic exposure upon well-studied, high aspect ratio SWCNTs and MWCNTs to asbestos on the subsequent aggressive behaviors and the underlying molecular mechanisms. Our results demonstrated for the first time aggressive transformation of human pleural mesothelial cells upon chronic exposure to CNTs and the role of MMP-2 in the process. This study strengthens the earlier finding on the mesothelioma pathogenicity of CNTs and supports the prudent adoption of prevention strategies and implementation of exposure control.

RESULTS

Chronic CNT Exposure Induces Cell Proliferation and Aggressive Behaviors of Mesothelial Cells. Nontumorigenic human lung mesothelial MeT5A cells were continuously exposed to subcytotoxic concentration (0.02 μg/cm^2) of SWCNTs, MWCNTs, crocidolite asbestos, or vehicle control for up to 4 months as described in Materials and Methods. This relatively low concentration was relevant to lung burdens achieved after *in vivo* exposure of mice to CNTs.[19−21] The exposed cells were evaluated for their growth characteristics by Cyquant cell proliferation and Hoechst 33342 assays and for their aggressive behaviors by Transwell cell migration and invasion assays. Analysis of cell growth characteristics by Cyquant assay shows that mesothelial cells treated with SWCNTs, MWCNTs, or asbestos exhibited a significantly higher growth rate than Survanta (vehicle)- or saline-treated controls (Figure 1A). Microscopic analysis of the cells by Hoechst assay confirmed the above finding (Figure 1B) and indicated that long-term exposure of mesothelial cells to SWCNTs, MWCNTs, or asbestos induced cell growth. The increase in cell growth was not observed until after 16 weeks of exposure.

The aggressive behaviors of particle-exposed cells were assessed by cell invasion and migration assays. Both SWCNT- and MWCNT-exposed cells demonstrated a significant increase in cell invasion (5.4- to 6.3-fold) and migration (2.5- to 2.7-fold) as compared to Survanta-treated control (Figure 1C,D). Likewise, asbestos-exposed cells exhibited an increase in cell motility as compared to saline-treated control but to a lesser extent than the SWCNT- and MWCNT-exposed cells. These results indicate that high aspect ratio SWCNTs and MWCNTs, like asbestos, can induce accelerated cell growth and invasiveness, which are key cancer phenotypes that may contribute to their mesothelioma pathogenicity.

Increased MMP-2 Expression and Activity in CNT-Transformed Mesothelial Cells. To understand the underlying mechanism of CNT-induced cell invasiveness, we investigated 12 selected genes known to be involved in the regulation of cell migration and invasion, including *CAV1*, *COL4A2*, *MMP-9*, *MMP-2*, *RAC1*, *STAT3*, *MET*, *NME1*, *SERPINE1*, *TIMP1*, *AKT1*, and *MAPK3* by quantitative real-time PCR (qPCR). Among these, *MMP-2* (also known as gelatinase A) was found to be most strikingly up-regulated in both SWCNT- and MWCNT-transformed cells as compared to control cells. In SWCNT cells, a 51-fold increase in *MMP-2* mRNA expression level was observed, whereas a 23-fold increase was seen in MWCNT cells (Figure 2A). Other genes that

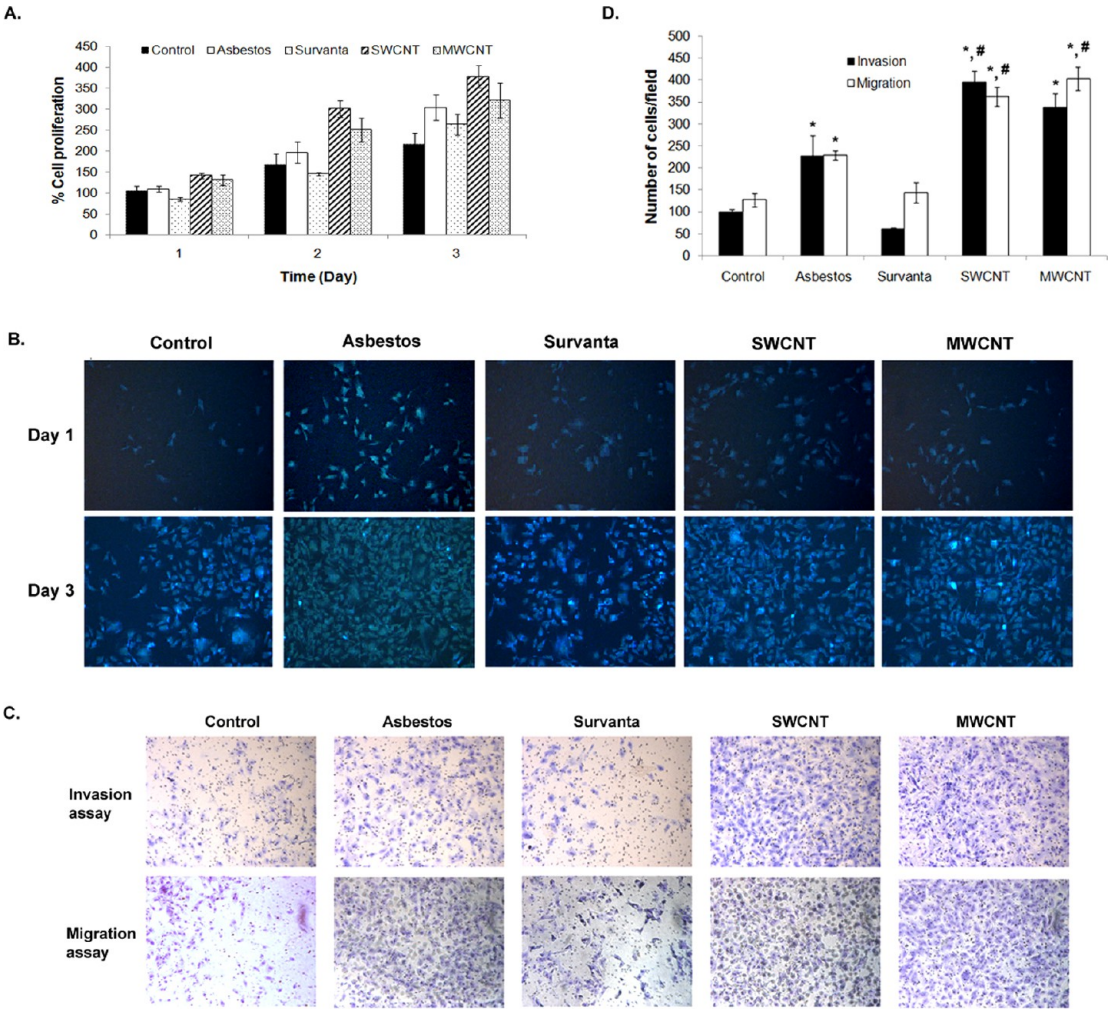

Figure 1. Chronic exposure to SWCNTs, MWCNTs, and asbestos induces cell proliferation and aggressive behavior of mesothelial MeT5A cells. (A) Passage control (Control), vehicle control (Survanta), and chronic SWCNT, MWCNT, or asbestos-exposed cells were seeded in a 96-well plate, and cell proliferation assay was performed using Cyquant cell proliferation kit for 3 continuous days. (B) Hoechst 33342 vital stain of passage control, vehicle control, and chronic SWCNT, MWCNT, or asbestos-exposed cells at 1 and 3 days after seeding. (C) Cell invasion and migration of passage control, vehicle control, and chronic SWCNT, MWCNT, or asbestos-exposed cells were determined using a Transwell with 8 μm pore size polycarbonate filter and a BD Matrigel invasion chamber. Cells that invaded or migrated to the lower side of the membrane were stained. (D) Invading and migrating cell numbers were then quantified by counting and depicted as bar charts; * = significant difference from control with $P < 0.05$, # = significant difference from asbestos-exposed cells with $P < 0.05$.

were slightly or moderately up-regulated in these cells include *CAV1*, *SERPINE1*, *TIMP1*, *AKT1*, and *MAPK3*. In asbestos-transformed cells, *MMP-2* and *SERPINE1* were most strongly up-regulated, followed by *CAV1* and *AKT1* (Figure 2B).

On the basis of its high expression profile in both CNT- and asbestos-transformed cells, we further investigated MMP-2. MMP-2 protein expression and gelatinolytic activity in SWCNT, MWCNT, and asbestos cells were examined by Western blotting, gelatin zymography, and immunofluorescence. Consistent with the mRNA expression data, MMP-2 protein expression and gelatinolytic activity were up-regulated in SWCNT, MWCNT, and asbestos-transformed cells (Figure 3A,B). Immunofluorescence staining of MMP-2 in these cells showed increased fluorescence intensity in SWCNT, MWCNT, and asbestos cells (136.1, 112.4, and 97.1 units/square inches, respectively) over control levels (94.5 and 61.8 units/square inches) in Survanta and saline-treated control cells (Figure 3C).

Gene Signaling Network Analysis Reveals the Importance of MMP-2 in CNT-Induced Invasion of Mesothelial Cells. To gain an insight into gene signaling contributing to the invasive phenotype of CNT and asbestos-transformed cells, whole genome microarray analysis of the cells was conducted and analyzed for gene signaling networks (GSNs) by Ingenuity Pathway Analysis (IPA). GSNs for cell invasion of SWCNT and MWCNT cells were very similar and are shown in Figure 4A. Interestingly, *MMP-2* occupied a focal position of the GSNs in both CNT- and asbestos-transformed cells. Other signaling hub genes with a first-order connection to *MMP-2* in the invasion GSNs include *PLAU*, *STAT3*, *AKT1*, and *VEGFA*. Invasion GSN of asbestos-transformed cells was

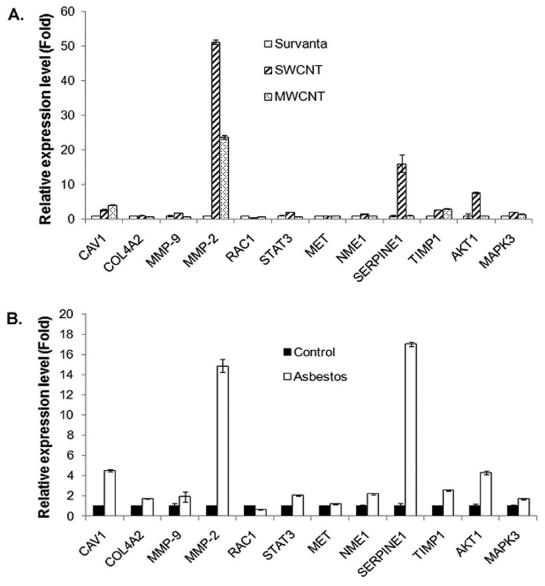

Figure 2. Elevation of cell invasion and migration regulatory genes in chronic CNT-exposed and asbestos-exposed MeT5A cells. Total RNA was isolated from passage control, vehicle control, and chronic SWCNT, MWCNT, or asbestos-exposed cells before reverse transcribed into cDNA. The expression of 12 selected genes reported to be involved in cell invasion and migration process including *CAV1*, *COL4A2*, *MMP-9*, *MMP-2*, *RAC1*, *STAT3*, *MET*, *NME1*, *SERPINE1*, *TIMP1*, *AKT1*, and *MAPK3* was analyzed by RT-qPCR. The relative expression of each gene to housekeeping gene *18S* in (A) chronic CNT-exposed cells and (B) chronic asbestos-exposed cells compared to vehicle control and passage control cells, respectively, is shown.

distinct and indicated *CAV1* and *CCL2* up-regulation and *EGFR* and *TIMP2* down-regulation (Figure 4B). *CAV1* and *CCL2* were however common hub genes found in the invasion GSNs of both CNT and asbestos cells. These results provide molecular evidence supporting the invasive properties of CNT and asbestos-transformed cells through some common and distinct gene signaling pathways.

Knockdown of MMP-2 Reduces the Invasiveness of CNT-Transformed Mesothelial Cells. To demonstrate the functional role of MMP-2 in the invasiveness of CNT-transformed cells, gene knockdown experiments were conducted in SWCNT, MWCNT, and asbestos-transformed cells. The cells were stably transfected with MMP-2 short-hairpin (sh)RNA plasmid and analyzed for MMP-2 gene and protein expression as well as gelatinase activity by qPCR, Western blotting, gelatin zymography, and immunofluorescence. Real-time PCR analysis of mRNA expression showed a substantial (73−82%) reduction in *MMP-2* mRNA in the shRNA-transfected SWCNT, MWCNT, and asbestos-transformed cells as compared to their respective controls (Figure 5A). Western blot and gelatin zymography studies similarly indicated a reduction in MMP-2 protein expression and enzyme activity in the shRNA-transfected cells (Figure 5B,C). Immunofluorescence studies further showed a corresponding reduction in MMP-2 immunofluorescence intensity in the three shRNA-transfected cells *versus* controls (Figure 5D). Together, these results indicate effective knockdown of MMP-2 expression and enzyme activity in the SWCNT, MWCNT, and asbestos-transformed mesothelial cells.

To determine whether MMP-2 plays a role in the aggressive behavior of CNT and asbestos-transformed cells, cell invasion and migration assays of the MMP-2 knockdown and vector-transfected control cells were performed. A substantial (60−90%) decrease in cell invasion was observed with the MMP-2 knockdown cells as compared to control cells (Figure 6A). Likewise, knocking down of MMP-2 in the CNT and asbestos-transformed cells has an inhibitory effect on the migratory activity of the cells (Figure 6B).

DISCUSSION

Pleural mesothelioma is one of the most aggressive forms of cancer that develops from transformed mesothelial cells originating in the pleura, the protective lining of the lungs and internal chest wall. The objective of this study was to investigate the effect of long-term exposure to subcytotoxic dose of CNTs on the aggressive behavior of human mesothelial cells, the pleural lining cells which have been reported to be strongly reactive in response to fiber exposure.[22] Here, we compared a set of well-studied SWCNT and MWCNT high aspect ratio particles to asbestos, a positive control HARN particle, for their abilities to cause aggressive behavior in human mesothelial cells. CNTs and other HARNs have been reported to be translocated to the pleural space, and their inadequate clearance from this site is considered a key determinant of their pathogenicity.[23] We demonstrated here for the first time that chronic exposure of human pleural mesothelial cells to CNTs induces proliferative and aggressive phenotypes of the cells, as indicated by their increased growth rate, migration, and invasion (Figure 1). Proliferative and genetic changes after cellular entry of SWCNTs and MWCNTs both *in vitro* and *in vivo* have been reported through a variety of mechanisms. One of these mechanisms is the interaction between the nanotubes and structural elements of the cell with apparent binding to the cytoskeleton, telomeric DNA, and G−C-rich DNA sequences in the chromosomes.[24,25] A study of lung epithelial cells exposed to CNTs demonstrated multipolar mitotic spindles, fragmented centrosomes, and aneuploid chromosomes. The increased multipolar mitotic spindles were associated with an increased number of cells in the G2 phase of mitosis leading to increased proliferation of CNT-exposed cells. These genetic alterations may be transmitted to daughter cells and have been suggested to be important in both tumorigenesis and tumor progression.[26] In the case of asbestos, it was reported to cause cell injury and induce a transient proliferative

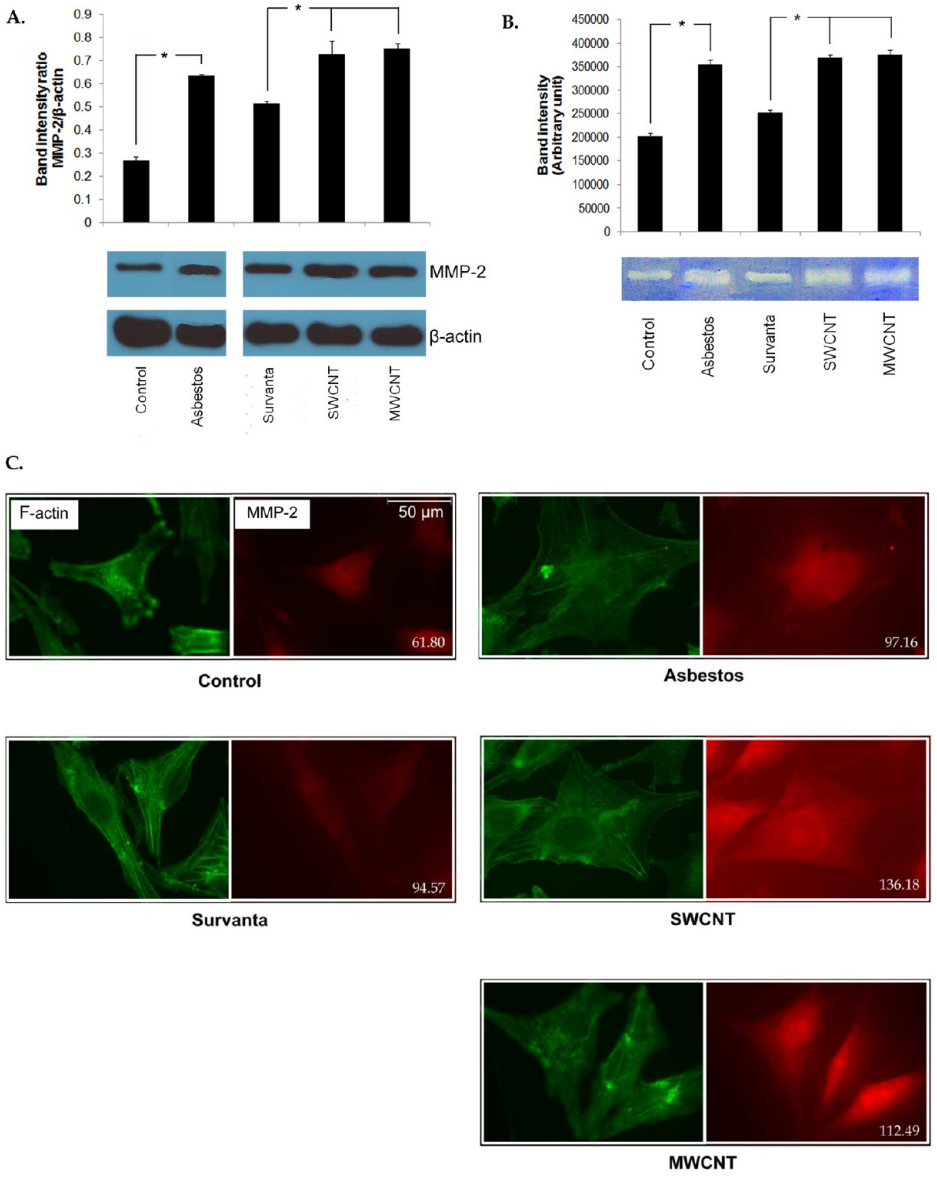

Figure 3. Increased MMP-2 expression and activity in chronic CNT-exposed and asbestos-exposed MeT5A cells. (A) MMP-2 expression in passage control, vehicle control, and chronic SWCNT, MWCNT, or asbestos-exposed cells was determined by Western blotting. Lysates of each sample were resolved under denaturing conditions by 10% SDS-PAGE and transferred onto PVDF membrane. The membrane was then probed with MMP-2 antibody and detected by an enhanced chemiluminescence detection system; * = significant difference with $P < 0.05$. (B) MMP-2 gelatinolytic activity of passage control, vehicle control, and chronic SWCNT, MWCNT, or asbestos-exposed cells was shown by gelatin zymography. Cell supernatants were collected, resolved by electrophoresis in SDS-polyacrylamide gels containing 0.1% gelatin, and stained with 0.5% Coomassie brilliant blue. Densitometry was used to compare enzymatic activity; * = significant difference with $P < 0.05$ (C). Cellular MMP-2 expression was visualized by immunofluorescence staining. Cells were cultured on glass coverslips, fixed in 4% paraformaldehyde, and stained for F-actin (green) and MMP-2 (red). MMP-2 expression level represented by red fluorescence intensity per square inch of each sample is indicated at the lower right corner of each capture.

response in mesothelial cells after a single exposure. Moreover, repeated exposures may induce prolonged injury, cytokine production, and mesothelial proliferation without necessarily involving direct action of asbestos fibers on these cells at the pleura.[27] Oxidative stress induction has also been implicated to trigger cell proliferation and injury upon asbestos exposure. The high iron content of asbestos fibers appeared to be critical to the genesis of reactive oxygen species (ROS), including the highly DNA-damaging hydroxyl radical. These reactive species can initiate aberrant transcriptional responses leading to the increase in cell proliferation and transformation.[28] An increase in ROS production along with the depletion and loss of protective mechanism against ROS in lung cells upon CNT exposure has been demonstrated, as well. This incidence has been linked to CNT-induced inflammation, genetoxicity, fibrosis, and granuloma formation in

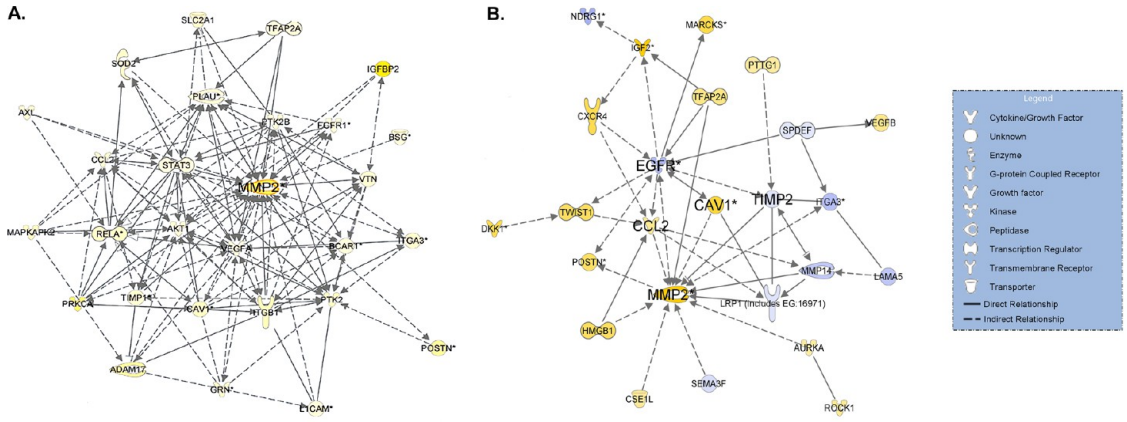

Figure 4. Invasion gene signaling networks (GSNs) of (A) chronic CNT-exposed and (B) chronic asbestos-exposed MeT5A cells. Whole genome expression for each treatment was determined using high-throughput mRNA microarray analysis. Differentially expressed genes (DEGs) were analyzed using Ingenuity Pathway Analysis (IPA) to create proinvasion GSN. Yellow and blue represent up- and down-regulation, respectively, compared to passage control or vehicle control cells. Color intensity signifies fold change.

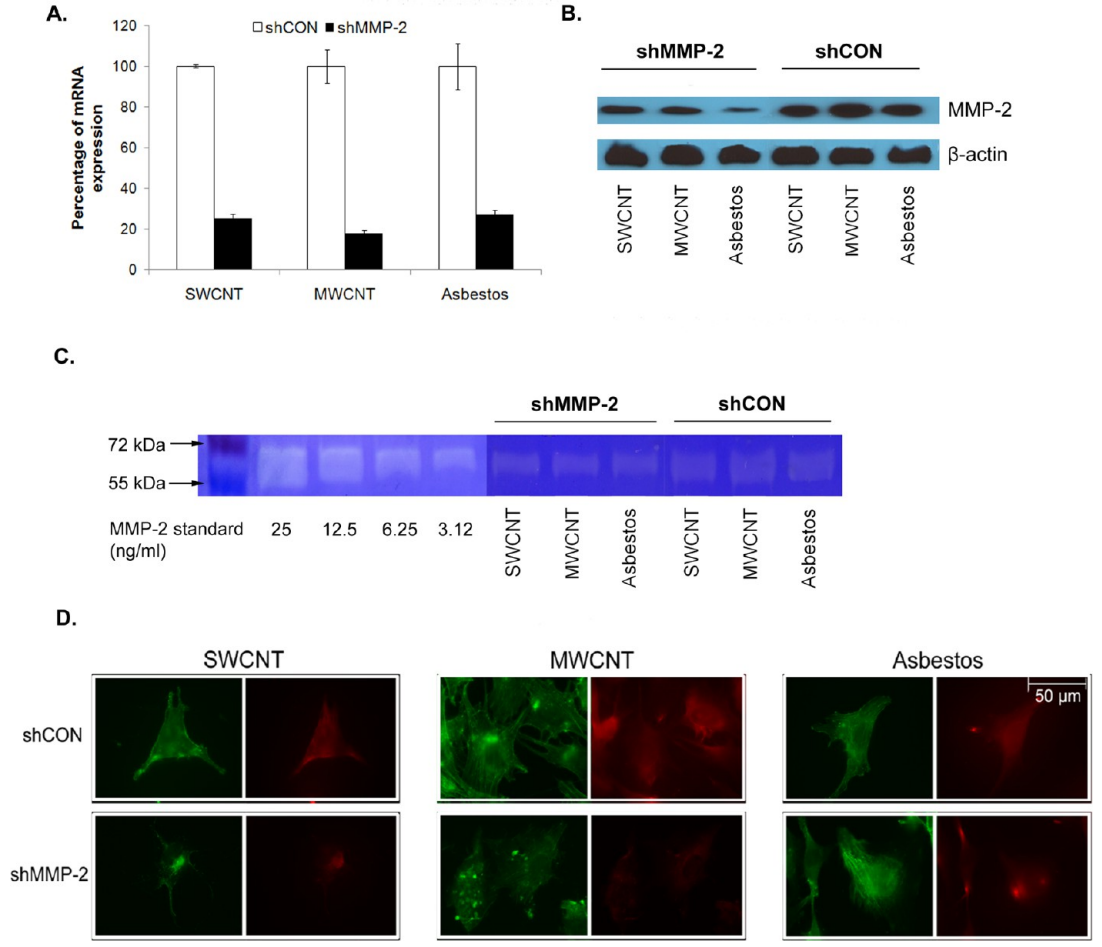

Figure 5. MMP-2 knockdown by shRNA transfection decreases MMP-2 expression and activity in chronic CNT-exposed and asbestos-exposed MeT5A cells. Cells were transfected with predesigned MMP-2 shRNA (shMMP-2) or scrambled vector (shCON). Stable MMP-2 knockdown clones were generated by puromycin selection. The knockdown efficiency was determined as MMP-2 gene and protein expression of shMMP-2-transfected cells compared to shCON-transfected cells by (A) qPCR and (B) Western blot analysis. (C) Gelatinase activity of shMMP-2-transfected and shCON-transfected cells demonstrated by gelatin zymography. (D) Immunofluorescence studies further showed the reduction of MMP-2 immunofluorescence intensity in the three shMMP-2-transfected cells compared to shCON-transfected cells. F-actin and MMP-2 were stained green and red, respectively.

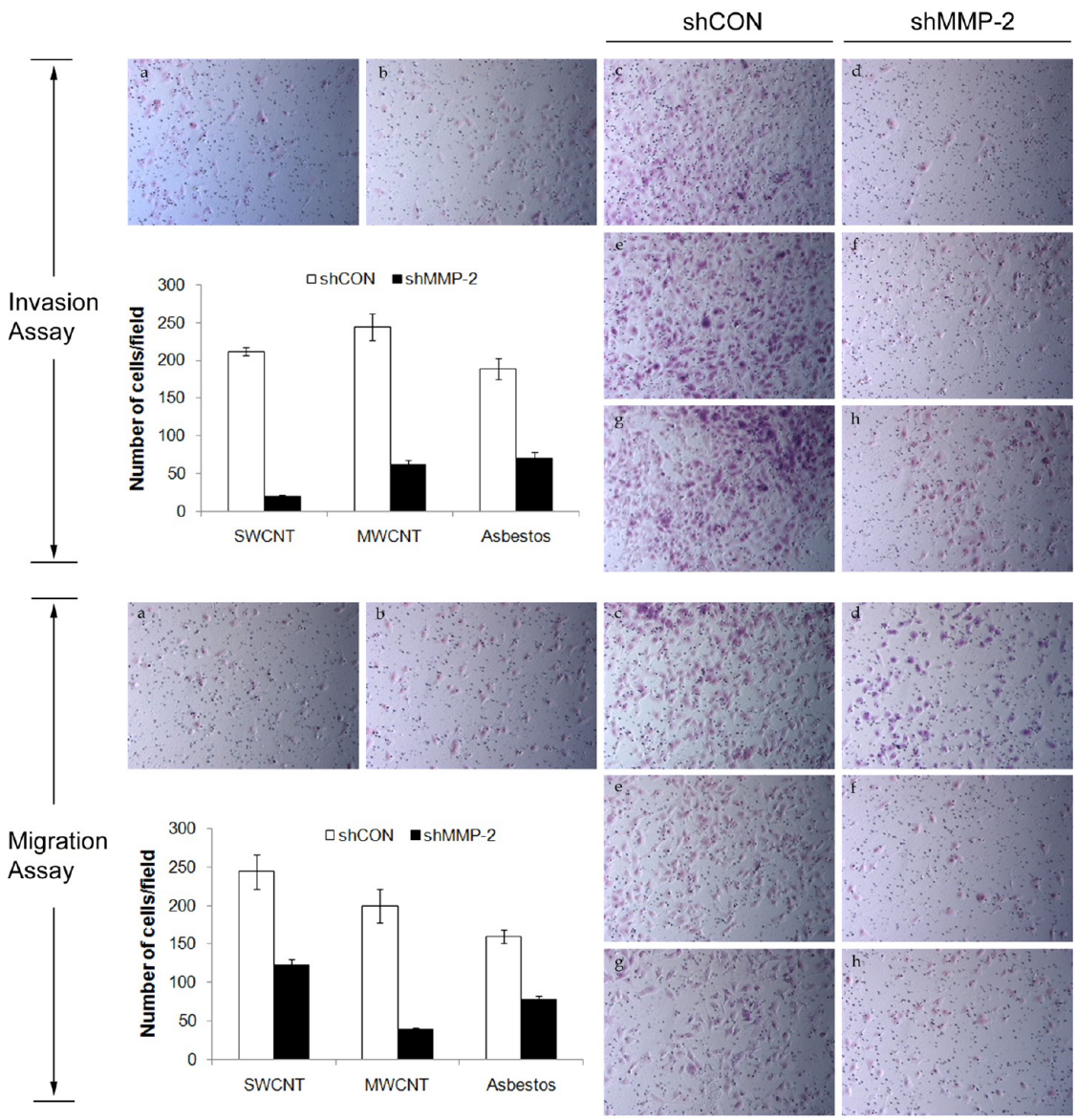

Figure 6. Effects of MMP-2 knockdown on the invasive and migratory activities of chronic CNT-exposed and asbestos-exposed MeT5A cells. Cell invasion and migration of shMMP-2-transfected and shCON-transfected cells were determined using Transwell cell invasion and migration assays. Cells that invaded or migrated to the lower side of the membrane were stained and counted. The number of invading and migrating cells per field was quantified and shown in the bar charts; a = passage control, b = vehicle control (Survanta), c and d = SWCNT-exposed cells, e and f = MWCNT-exposed cells, g and h = asbestos-exposed cells.

mice.[29] Consistently, our 4 month CNT- and asbestos-exposed cells exhibit increased ROS production and reduced superoxide dismutase-1 (SOD-1) expression (Supporting Information) Figure S1.

Increased cell invasion and migration were observed in mesothelial cells chronically exposed to CNTs and asbestos (Figure 1B). Cell migration and invasion are crucial steps in many physiological events such as embryogenesis, morphogenesis, angiogenesis, wound healing, and inflammation. However, cell migration and invasion are also implicated in many pathological processes, such as carcinogenesis and metastasis, and have been used to assess the aggressive and malignant phenotypes of the cells.[30,31] We previously reported the malignant transformation and tumorigenesis of human lung epithelial cells after long-term exposure to SWCNTs as well as the induction of cancer phenotypes including cell invasion and migration, but the genes involved in the increased migration and invasion are not known.[32] Meanwhile, asbestos-induced mesothelioma, a highly invasive type of cancer, has been reported to express high levels of growth factor receptor and oncogenes especially *c-FOS* and *c-JUN*.[33] Ultrafine carbon black (UFCB) was used as a comparative non-HARN particle in this study. With the same dispersion method as CNTs, long-term UFCB exposure induced mesothelial cell growth equivalent to CNTs and asbestos (Supporting

Information Figure S2A). This is in conformity with the previously reported stimulatory effect of UFCB on human airway epithelial cell proliferation *via* the process of soluble proheparin-binding (HB)-EGF release and concomitant activation of epidermal growth factor receptor (EGFR) and ERK cascade.[34] Although UFCB could stimulate cell proliferation, the effect on cell invasion and migration was significantly lower than that for SWCNTs and MWCNTs (Supporting Information Figure S2B,C). Thus, UFCB-exposed cells were excluded from further study.

Since migration and invasion of cells through tissues is a highly coordinated process that involves several interdependent steps and various specific genes,[35] we tested 12 selected genes most frequently associated with cell migration and invasion using RT-qPCR (Figure 2). Both SWCNT and MWCNT-exposed cells exhibited a dramatic increase in *MMP-2* expression, which is the highest among the genes tested. Increased MMP-2 protein expression and gelatinolytic activity were also observed with the CNT-exposed cells, as determined by Western blotting, immunofluorescence, and gelatin zymography (Figure 3). Several MMP genes have been reported to be up-regulated in mice after pulmonary CNT exposure and have been shown to be associated in early lung fibrotic and subchronic tissue damage induction.[36,37] *MMP*s are signature invasion marker genes that encode proteins involved in the degradation of ECM and are typically highly active during lung cancer development and progression.[38] *MMP-2* is also highly up-regulated in cells chronically exposed to asbestos (Figure 3). This finding is consistent with a previous report showing an increase in *MMP-2*, *MMP-7*, *MMP-9*, *MMP-12*, and *MMP-13* expression in the lungs of mice after intratracheal instillation of asbestos and suggests the contribution of MMPs on asbestos-induced lung inflammation and fibrosis, particularly *MMP*-2, which is increased in the fibrotic phase and also in the fibrotic region.[39]

It is known that degradation and remodeling of ECM are essential to cell migration, invasion, and metastasis. These processes are mediated by several proteolytic enzymes, most notably MMPs.[40] MMPs belong to a family of zinc-dependent endopeptidases, highly conserved and structurally related enzymes capable of degrading many components of basement membrane and ECM.[41] They can be divided into different classes according to their sequence homology, substrate specificity, and cellular localization. The 72 kDa MMP-2 (gelatinase A) has an important role in basement membrane turnover due to its specific activity to collagen type IV or gelatin which is the major structural protein of the basement membrane. Its degradation plays a role in cell invasion of the vasculature and is considered to have a key role in metastasis. *MMP-2* expression has been associated with the invasiveness of many cancer cell lines and is elevated in high-grade tumors, specifically at the invasive front and in vascular invasion.[42,43] Inhibition of MMP-2 activity by MMP-2 inhibitors has been reported to suppress local invasiveness of various carcinomas.[44−46] Furthermore, elevated MMP-2 levels have been used for prognosis of invasive and metastatic lung cancers, and the reduction of cancer cell colonization in the lung of MMP-2-deficient mice than wild-type mice has been reported.[47]

Whole genome microarray and IPA were used to hypothesize proinvasion gene networks of chronic CNT- and asbestos-exposed mesothelial cells (Figure 4). The importance of *MMP-2* in both CNT- and asbestos-induced networks is indicated by focal position of MMP-2-encoded genes in both networks with a slight difference in some associated hub genes. In a CNT-induced proinvasion network, other signaling hub genes with first-order linkage to *MMP-2* include *PLAU*, *STAT3*, *AKT1*, and *VEGFA*. Urokinase-plasminogen activator or *PLAU* gene is known to encode uPA, the protease which degrades ECM and plays critical roles in cell migration, tissue remodeling, angiogenesis, tumor invasion, and metastasis.[48,49] Plasminogen activators convert plasminogen to plasmin, which works more efficiently in proteolysis of the fibrin, whereas the MMPs' family is the main proteases for fibronectin, laminin, elastin, and collagens. In addition, plasminogen activators activate several MMPs and could also facilitate the MMPs' activities. The overlapping contribution of uPA and MMP-2 in cell migration and invasion has been reported to be correlated with more aggressive metastatic behavior of cancer cells.[50] *STAT3* has been shown to regulate tumor growth, angiogenesis, and metastasis of several cancer types including non-small cell lung cancer and mesothelioma. *STAT3* activation is also contributed to oncogenesis. The role of activated *STAT3* in oncogenesis is manifested presumably through its role in the expression of many key genes that regulate multiple aspects of tumor cell survival, growth, angiogenesis, and evasion of immune surveillance such as *cyclin D1*, *c-myc*, *vascular endothelial growth factor* (*VEGF*), and *IP-10*.[51] Several studies have shown that *MMP-2* transcription is directly regulated by *STAT3*. It has been reported that *STAT3* can bind to the promoter of *MMP-2* gene and up-regulates its expression. Blockade of activated *STAT3* by ectopic expression of dominant negative *STAT3* suppresses *MMP-2* expression and invasiveness of tumor cells, inhibits tumor growth, and prevents metastasis in nude mice.[52,53] Phosphatidylinositol-3-kinase (*PI3K*)-*AKT* signaling plays a prominent role in several processes considered the hallmark of cancer. It has been reported that *AKT* promotes cancer cell invasion *via* increased motility and MMP

production. MMP-driven metastasis has also been reported to correlate with phosphorylation of ERK1/2 and PI3K/AKT. *AKT1* is one of three mammalian isoforms and is activated by several growth factor pathways and implicated in a variety of cellular functions, such as survival, transcription, and translation. The correlation between invasion activity of *AKT1* expressing cells and the increase of MMP-2 expression and activation has been reported. It was suggested that the invasive behavior induced by *AKT1* may result from inhibition of MMP-2 degradation by the proteasome pathway.[54,55] *VEGF* is a well-known regulator of tumor progression, angiogenesis, and metastasis. Positive correlation between *VEGF* and *MMP-2* expression has been reported in lung carcinoma cells. MMP-2 has been found to regulate the production of VEGF, and VEGF overexpression may promote the expression of MMP-2, as well.[56] For the asbestos-induced proinvasion network, the important upstream genes that may regulate MMP-2 production are *CAV1*, *TIMP2*, and *CCL2*. Down-regulation of tissue inhibitor of MMP-2 (TIMP-2) is shown in the network. An imbalance between the proteolytic activity of MMP-2 and TIMP-2 is responsible for the degradation of ECM components, a key step in tumor invasion and metastasis. Several studies have reported that the invasion and metastasis dissemination is facilitated by increased levels of MMP-2 and/or decreased levels of TIMP-2, either of which can shift the balance of proteolysis or cause basement membrane degradation. This is the key point for the beginning of tumor spread and metastasis formation, which have a positive correlation with MMP-2 proteolytic activity.[57−59] *CAV1* and *CCL2* are overexpressed in both CNT and asbestos-induced proinvasion GSN. Caveolin-1 (CAV1) is a major component of cell surface invagination caveolae which could interact with many signal molecules such as EGFR, IR, and PDGF receptor and play an important role in cell adhesion and growth-factor-mediated signal transduction. Recently, *CAV1* has been identified as a metastasis-associated gene, and *CAV1* up-regulation is associated with highly migratory and invasive cancer cells *via* the induction of MMP-9 production and MMP-2 activation.[60] Monocyte chemoattractant protein-1 (MCP-1) encoded by *CCL2* gene is an inflammatory biomarker known to be overproduced after asbestos and CNT exposure. Induction of MCP-1 mRNA expression in rat pleural mesothelial cells after crocidolite and chrysotile asbestos exposure and the increase of MCP-1 protein in the pleural lavage fluid of exposed rats have been reported.[61] Significant elevations of several cytokines and chemokines including MCP-1 in bronchoalveolar lavage fluid were also noted after pharyngeal instillation.[62] Cell migration and invasion driven by MCP-1 has been described, and several studies revealed that MCP-1 could enhance MMP-2 activity.[63] Further examination of microarray data showed the increase of oxidative phosphorylation reactions associated with mitochondrial metabolism function which correlated with the increase of ROS production and reduction of SOD-1 expression in both CNT- and asbestos-exposed cells. Since ROS was known to activate several upstream pathways that mediate MMP-2 activity *via* different signal molecules and genes including *AKT1* and MCP-1 which were found to be up-regulated in CNT- and asbestos-induced proinvasion GSN,[64,65] oxidative stress induction may be a factor involved in CNT- and asbestos-induced MMP-2 activation.

To confirm the importance of MMP-2 in cell migration and invasion caused by chronic exposure to CNTs and asbestos, SWCNT, MWCNT and asbestos-transformed cells were transfected with MMP-2 shRNA or control plasmid, and MMP-2 mRNA and protein expression as well as enzyme activity were determined by qPCR, Western blotting, immunofluorescence, and gelatin zymography (Figure 5). As compared to control transfectants, all MMP-2 shRNA transfectants exhibited substantially reduced MMP-2 expression and activity. Functionally, the MMP-2 knockdown cells showed greatly reduced invasive and migratory properties as compared to their vector-transfected controls (Figure 6). Collectively, the observation that MMP-2 is up-regulated in all CNT- and asbestos-exposed cells and the finding that down-regulation of MMP-2 in these cells consistently inhibits their aggressive behaviors suggest a common and important role of MMP-2 in HARN-induced mesothelial toxicities. Due to concerns over rapid development of new nanomaterial technologies and the risks to human health, this long-term *in vitro* exposure model can provide rapid, robust, and high-throughput assessments for future research on mesothelioma hazard of nanomaterials.

CONCLUSION

In summary, we demonstrated that chronic exposure of human pleural mesothelial cells to CNTs or asbestos induced cell transformation with cancer-like properties such as rapid growth and increased cell invasion and migration. The described *in vitro* exposure model could potentially be used to predict mesothelioma pathogenicity of nanomaterials and to aid mechanistic studies of the cellular and molecular events leading to mesothelioma. Using the described model, we identified several genes involved in the transformation and aggressive behaviors of chronic CNT and asbestos-exposed mesothelial cells. Among these, MMP-2 was identified as a key regulator of the aggressive behaviors of the transformed cells based on gene expression and knockdown data. Gene signaling networks obtained from microarray data and IPA confirmed the importance of MMP-2 in cell invasion

induced by chronic CNT and asbestos exposure. Other genes involved in the CNT-induced invasion network include *PLAU*, *STAT3*, *AKT1*, and *VEGFA*, whereas *CAV1*, *EGFR*, *TIMP2*, and *CCL2* are altered in the asbestos-induced invasion network. These genes have the potential to regulate MMP-2 production and activity in CNT and asbestos-transformed cells.

MATERIALS AND METHODS

Cell Culture and Chronic Exposure. Human pleural mesothelial MeT5A cells were acquired from American Type Culture Collection (Manassas, VA) and maintained in M199 medium (Life Technologies, Grand Island, NY) with 5% fetal bovine serum (FBS), 2 mM L-glutamine, 100 U/mL penicillin/streptomycin, 1 μg/mL EGF, and 50 μg/mL hydrocortisone. Cell cultures were performed in a humidified atmosphere of 5% CO_2 at 37 °C. SWCNTs, synthesized using high-pressure carbon monoxide disproportionate process (HiPCO), were obtained from Carbon Nanotechnology (CNI, Houston, TX). MWCNTs were provided by Mitsui & Company (MWNT-7, lot #05072001K28), and crocidolite asbestos (CAS# 12001-28-4) was obtained from the Kalahari Desert in South Africa by the National Institute of Environmental Health Sciences (Research Triangle Park, NC). UFCB was acquired from Cabot (Edison, NJ). All tested particles were characterized as previously described in our recent study.[66] Elemental analysis of the supplied SWCNTs by nitric acid dissolution and inductively coupled plasma atomic emission spectrometry (ICP-AES, NMAM #7300) showed that SWCNTs were 99% elemental carbon and contained less than 1% w/w of contaminants, while MWCNTs contained 0.41% w/w metal impurity. Both SWCNTs and MWCNTs possessed ≤0.32% Fe and ≤0.41% Na ion impurities. Diameter and length distribution of dispersed particles were measured by field emission scanning electron microscopy (FESEM, model S-4800; Hitachi, Tokyo, Japan). Mean lengths of SWCNTs, MWCNTs, and asbestos were 1.42, 4.90, and 10 μm, while mean widths were 0.38, 0.08, and 0.21 μm, respectively. UFCB possessed <1% w/w metal impurities with a dry and medium dispersed width of 37 and 700 nm, respectively. All particles possessed surface areas between 9.8 and 43 m^2/g except SWCNT, which was 10- to 100-fold greater (400−1040 m^2/g).

The cells were continuously exposed to a subcytotoxic concentration (0.02 $\mu g/cm^2$) of SWCNTs, MWCNTs, crocidolite asbestos, UFCB, or vehicle for 4 months following the method previously described.[67] Briefly, 0.1 mg/mL stocks of SWCNTs and MWCNTs in phosphate buffer saline (PBS) containing 150 μg/mL Survanta (Abbott Laboratories, Abbott Park, IL) were sonicated and diluted in media (0.1 μg/mL) prior to cell exposure. This method of dispersion mimics natural lung surfactant content, is nontoxic, and is effective in dispersing CNTs to the size of aerosolized particles reported in the workplace.[68] Crocidolite asbestos was sonicated in culture medium without the dispersant. MeT5A cells (1×10^4) were exposed to the dispersed particles every 3 days following a PBS wash and passaged once per week to initial seeding densities. Vehicle-only exposed cells and passage-matched control cells were used as controls. Calculation of the exposure dose was based on *in vivo* SWCNT and MWCNT aspiration and inhalation total lung burden dose of 20 μg/mouse previously reported.[69] The penetration of CNTs from lung periphery through the visceral pleura into the pleural space after aspiration exposure has been quantified and 0.6% of the deposited fiber burden was found to reach the visceral pleura. From the estimated pleural surface area of 5 cm^2 in mice, the possible dose of CNT per cm^2 of visceral pleura is approximately 0.024 $\mu g/cm^2$.

Cell Proliferation Assays. Cell proliferation was quantified over a 72 h period using Cyquant cell proliferation assay kit (Invitrogen, Grand Island, NY) and Hoechst 33342 vital staining. In the Cyquant assay, cells were seeded (5000 cells/well) in quadruplicate in a 96-well plate in a normal growth medium. Cells were incubated for various times before the replacement of media with 100 μL of 1× Cyquant dye solution and incubated for 1 h. Each sample's fluorescence intensity was measured using a fluorescence microplate reader at a 485 nm excitation and 520 nm emission (FLUOstar OPTIMA, BMG Labtech, Durham, NC). In the Hoechst assay, 10 mg/mL stock solution of Hoechst 33342 was diluted to 5 μg/mL in PBS, and 100 μL of the 5 μg/mL solution was added into each well. The cells were incubated for 30 min before visualization under a fluorescence microscope (Leica Microsystems, Bannockburn, IL).

Migration and Invasion Assays. Cell migration and invasion were determined in the 24-well plate Transwell system with 8 μm pore size polycarbonate filter and BD Matrigel invasion chamber (BD Biosciences, NJ). Briefly, cells at the density of 1.5×10^4 cells per well (migration) or 3×10^4 cells per well (invasion) were seeded into the upper chamber of the Transwell unit in serum-free medium. The lower chamber of the unit was added with a normal growth medium containing 5% FBS. The unit was incubated at 37 °C in a 5% CO_2 atmosphere for 48 h. The nonmigrating or noninvading cells were removed from the inside of the insert with a cotton swab. Cells that migrated or invaded to the lower side of the membrane were fixed and stained with Diff-Quik (Dade Behring, Newark, DE). Inserts were visualized and scored under a light microscope (Leica DM, IL).

Quantitative Real-Time PCR of Motility Genes. The expression of 12 selected genes known to be involved in the regulation of cell migration and invasion including *CAV1*, *COL4A2*, *MMP-9*, *MMP-2*, *RAC1*, *STAT3*, *MET*, *NME1*, *SERPINE1*, *TIMP1*, *AKT1*, and *MAPK3* was analyzed. Total RNA was isolated from cells using RNeasy mini kit (Qiagen, Valencia, CA), according to the manufacturer's instructions. The extracted RNA was then reverse transcribed into cDNA by high capacity RNA to cDNA kit (Applied Biosystems, Carlsbad, CA). After the reverse transcription reaction was finished, 10 μL of diluted cDNA product (final cDNA quantity 100 ng) was mixed with 10 μL of Taqman master mix (Applied Biosystems) and transferred into Taqman array plate (Applied Biosystems). Quantification of the PCR products was performed by NFQ-FAM method using the Applied Biosystems 7500 real-time PCR system with the following profile: 1 cycle at 94 °C for 2 min, 40 cycles at 94 °C for 15 s, 60 °C for 1 min, 72 °C for 1 min. Data analysis was performed using the ABI sequence detection software (Applied Biosystems) by relative quantification. The threshold cycle (C_t), which is defined as the cycle at which PCR amplification reaches a significant value, is given as the mean value. The relative expression of each mRNA was calculated by the ΔC_t method, where ΔC_t is the value obtained by subtracting the C_t value of the housekeeping gene *18S* mRNA from the C_t value of the target mRNA. The amount of the target relative to *18S* mRNA was expressed as $2^{-\Delta C_t}$.

Western Blot Analysis. Cells were washed twice with ice-cold PBS and incubated in lysis buffer containing 20 mM Tris-HCl (pH 7.5), 1% Triton X-100, 150 mM NaCl, 10% glycerol, 1 mM Na_3VO_4, 50 mM NaF, 100 mM phenylmethylsulfonyl fluoride, and a commercial protease inhibitor mixture (Roche Molecular Biochemicals, Indianapolis, IN) at 4 °C for 20 min. Cell lysates were collected and analyzed for protein content using the BCA protein assay kit (Pierce Biotechnology, Rockford, IL). Samples containing 50 μg of cell lysate proteins per lane were resolved under denaturing conditions by 10% sodium dodecyl sulfate-polyacrylamide gel electrophoresis (SDS-PAGE) along with EZ-run prestained protein ladder (Fisher Scientific, Pittsburgh, PA) and transferred onto PVDF membranes (Invitrogen, Carlsbad, CA). The transferred membranes were blocked for 1 h in 5% nonfat dry milk in TBST (25 mM Tris-HCl, pH 7.4, 125 mM NaCl, 0.05% Tween 20) and incubated with the appropriate primary antibodies at 4 °C overnight. Membranes were washed twice with TBST for 10 min and incubated with horseradish peroxidase-coupled isotype-specific secondary antibodies for 1.5 h at room temperature. The immune complexes were detected by

an enhanced chemiluminescence detection system (Amersham Biosciences, Piscataway, NJ) and quantified using analyst/PC densitometry software (Bio-Rad Laboratories, Hercules, CA).

Gelatinolytic Activity. Cells at the density of 1×10^5 cells/well were seeded into a 6-well plate with 1 mL of completed M199 medium and cultured for 24 h. Cell supernatants were collected and determined for total secreted protein concentrations and analyzed by zymography. Secreted proteins at 5 μg per lane were separated by electrophoresis in SDS-polyacrylamide gels containing 0.1% gelatin. After electrophoresis, gels were renatured by incubation in 2.5% Triton X-100 for 30 min, incubated overnight in substrate buffer (50 mM Tris-HCl, pH 7.5, containing 10 mM $CaCl_2$) at 37 °C, and stained with 0.5% Coomassie brilliant blue. Recombinant MMP-2 (Raybiotech, Norcross, GA) was used as a positive control. A clear zone in the blue background indicated the presence of gelatinolytic activity. Computerized densitometry was used to evaluate enzymatic activity.

Immunofluorescence Staining. Cellular MMP-2 expression was visualized by immunofluorescence microscopy (Zeiss LSM 510 Axiovert 100M, Zeiss, Thornwood, NY) as previously described.[70] Briefly, cells were cultured to confluence on glass coverslips and fixed in 4% paraformaldehyde in PBS. The samples were rinsed three times, permeabilized with 1.2% Triton X-100 for 5 min, rinsed three times, and blocked with 1% bovine serum albumin (BSA) in PBS for 1 h before staining with 1:200 MMP-2 primary antibody (Abcam, Cambridge, MA) followed by Alexa Fluor-conjugated secondary antibody (Invitrogen, Carlsbad, CA). The stained cells were mounted with ProLong gold antifade reagent with DAPI (Invitrogen, Carlsbad, CA) and visualized by fluorescence microscopy. All microscopic exposure conditions were set the same between samples for fluorescence intensity comparison using Image J Java-based image processing program. Fluorescence intensity per square inches was calculated.

Whole Genome Expression Microarray and Ingenuity Pathway Analysis. Whole genome expression for each treatment was determined using high-throughput mRNA microarray analysis following MIAME guidelines as described previously.[71] Briefly, cells from each treatment (1×10^6 in a 6 cm plate) were lysed in triplicate using TRIzol reagent (Life Technologies, Grand Island, NY). Total RNA was isolated, purified, and quantified using Nanodrop ND-1000 (Thermo Scientific, Rockford, IL). RNA was tested for purity and DNA contamination using A260/A280 ratio and standard denaturing agarose gel electrophoresis. Double-stranded cDNA was synthesized using Invitrogen Superscript ds-cDNA synthesis kit, cleaned, and Cy3-labeled by a NimbleGen One-Color DNA labeling kit following the manufacturer's protocol (Roche NimbleGen, Madison, WI). Samples were hybridized to NimbleGen Human 12 × 135k gene expression array using the NimbleGen hybridization system. The slides were then washed with NimbleGen wash buffer, dried, and scanned with Axon GenePix 4000B microarray scanner (Molecular Devices Corporation, Sunnyvale, CA). Finally, raw data intensities were extracted from the aligned scanned images and normalized through quantile normalization and robust multichip average method in NimbleGen v2.5. Gene level files were imported into Agilent GeneSpring GX (v12.1) for analysis. Genes with <50.0 intensity were removed from further analysis. Volcano plots were constructed using two sample *t*-tests assuming equal variance ($p \leq 0.05$) with a fold-change screening ($\geq \pm 2$-fold) to identify differentially expressed genes (DEGs) for SWCNTs and MWCNTs compared to dispersant-treated cells and asbestos compared to control cells. Microarray expression data were compared to qPCR invasion gene data to validate the microarray. All gene expression data were deposited to NCBI's Gene Expression Omnibus and is accessible *via* accession number (GenBank ID: GSE48855).

To investigate the impact of chronic CNT or asbestos exposure on gene signaling promoting invasive behavior, DEGs were analyzed using Ingenuity Pathway Analysis (IPA, version Fall 2012; Redwood City, CA). Tab-delimited text files containing gene IDs, expression data, and *t*-test *p* values were uploaded into IPA. Gene signaling networks (GSNs) associated with promoting invasion were created and mapped. Genes were included in the GSN if they promoted invasion and were overexpressed or if they inhibited invasion and were underexpressed.

MMP-2 Short-Hairpin RNA Transfection. Cells were transfected with predesigned MMP-2 shRNA or scrambled vector (SureSilencing, SAbiosciences, Frederick, MD) according to the manufacturer's protocol. Stable MMP-2 knockdown clones were generated by puromycin selection (0.2 μg/mL, Life Technologies, Grand Island, NY). Expression of MMP-2 in the shRNA and scrambled vector-transfected cells was determined by qPCR and Western blotting as described above.

Statistical Analysis. Results are expressed as means ± SD. All values were derived from at least three independent experiments. Differences between groups were assessed by one-way analysis of variance (ANOVA). If the variances between groups were homogeneous, groups were subjected to the multiple comparison Dunnett's test. If the variances were not homogeneous, groups were compared by the Mann−Whitney test. Differences were considered significant if *P* values were <0.05.

Conflict of Interest: The authors declare no competing financial interest.

Acknowledgment. This work was supported by grants from the National Science Foundation (EPS-1003907) and National Institutes of Health (R01-HL095579). Imaging experiments were performed in the West Virginia University Imaging Facility, which is supported in part by the Mary Babb Randolph Cancer Center and NIH Grants P20 RR016440, P30 RR032138/GM103488, and P20 RR016477. The findings and conclusions in this report are those of the authors and do not necessarily represent the views of the National Institute for Occupational Safety and Health.

Supporting Information Available: Supporting Figures S1 and S2. This material is available free of charge *via* the Internet at http://pubs.acs.org.

REFERENCES AND NOTES

1. Shvedova, A. A.; Kisin, E. R.; Porter, D.; Schulte, P.; Kagan, V. E.; Fadeel, B.; Castranova, V. Mechanisms of Pulmonary Toxicity and Medical Applications of Carbon Nanotubes: Two Faces of Janus? *Pharmacol. Ther.* **2009**, *121*, 192–204.
2. Helland, A.; Wick, P.; Koehler, A.; Schmid, K.; Som, C. Reviewing the Environmental and Human Health Knowledge Base of Carbon Nanotubes. *Environ. Health Perspect.* **2007**, *115*, 1125–1131.
3. Donaldson, K.; Murphy, F.; Schinwald, A.; Duffin, R.; Poland, C. A. Identifying the Pulmonary Hazard of High Aspect Ratio Nanoparticles To Enable Their Safety-by-Design. *Nanomedicine* **2011**, *6*, 143–156.
4. Elgrabli, D.; Floriani, M.; Abella-Gallart, S.; Meunier, L.; Gamez, C.; Delalain, P.; Rogerieux, F.; Boczkowski, J.; Lacroix, G. Biodistribution and Clearance of Instilled Carbon Nanotubes in Rat Lung. *Part. Fibre Toxicol.* **2008**, *5*, 20–32.
5. Donaldson, K.; Murphy, F. A.; Duffin, R.; Poland, C. A. Asbestos, Carbon Nanotubes and the Pleural Mesothelium: A Review of the Hypothesis Regarding the Role of Long Fibre Retention in the Parietal Pleura, Inflammation and Mesothelioma. *Part. Fibre Toxicol.* **2010**, *7*, 5–21.
6. Chou, C. C.; Hsiao, H. Y.; Hong, Q. S.; Chen, C. H.; Peng, Y. W.; Chen, H. W.; Yang, P. C. Single-Walled Carbon Nanotubes can Induce Pulmonary Injury in Mouse Model. *Nano Lett.* **2008**, *8*, 437–445.
7. Lam, C. W.; James, J. T.; McCluskey, R.; Hunter, R. L. Pulmonary Toxicity of Single-Wall Carbon Nanotubes in Mice 7 and 90 Days After Intratracheal Instillation. *Toxicol. Sci.* **2004**, *77*, 126–134.
8. Muller, J.; Huaux, F.; Moreau, N.; Mission, P.; Heilier, J. F.; Delos, M. Respiratory Toxicity of Multi-wall Carbon Nanotubes. *Toxicol. Appl. Pharmacol.* **2005**, *207*, 221–231.
9. Murphy, F. A.; Poland, C. A.; Duffin, R.; Donaldson, K. Length-Dependent Pleural Inflammation and Parietal Pleural Responses after Deposition of Carbon Nanotubes in the Pulmonary Airspaces of Mice. *Nanotoxicology* **2013**, *7*, 1157–1167.

10. Mercer, R. R.; Hubbs, A. F.; Scabilloni, J. F.; Wang, L.; Battelli, L. A.; Schwegler-Berry, D.; Castranova, V.; Porter, D. W. Distribution and Persistence of Pleural Penetrations by Multi-walled Carbon Nanotubes. *Part. Fibre Toxicol.* **2010**, *7*, 28–38.
11. Yang, H.; Testa, J. R.; Carbone, M. Mesothelioma Epidemiology, Carcinogenesis, and Pathogenesis. *Curr. Treat. Options Oncol.* **2008**, *9*, 147–157.
12. Puhakka, A.; Ollikainen, T.; Soini, Y.; Kahlos, K.; Saily, M.; Koistinen, P. Modulation of DNA Single-Strand Breaks by Intracellular Glutathione in Human Lung Cells Exposed to Asbestos Fibers. *Mutat. Res.* **2002**, *514*, 7–17.
13. Pacurari, M.; Yin, X. J.; Zhao, J.; Ding, M.; Leonard, S. S.; Schwegler-Berry, D.; Ducatman, B. S.; Sbarra, D.; Hoover, M. D.; Castranova, V.; *et al.* Raw Single-Wall Carbon Nanotubes Induce Oxidative Stress and Activate MAPKs, AP-1, NF-κB, and AKT in Normal and Malignant Human Mesothelial Cells. *Environ. Health Perspect.* **2008**, *116*, 1211–1217.
14. Kaiser, J. P.; Wick, P.; Manser, P.; Spohn, P.; Bruinink, A. Single Walled Carbon Nanotubes (SWCNT) Affect Cell Physiology and Cell Architecture. *J. Mater. Sci. Mater. Med.* **2008**, *19*, 1523–1527.
15. Tabet, L.; Bussy, C.; Amara, N.; Setyan, A.; Grodet, A.; Rossi, M. J.; Pairon, J. C.; Boczkowski, J.; Lanone, S. Adverse Effects of Industrial Multiwalled Carbon Nanotubes on Human Pulmonary Cells. *J. Toxicol. Environ. Health A* **2009**, *72*, 60–73.
16. Bozzuto, G.; Ruggieri, R.; Molinari, A. Molecular Aspects of Tumor Cell Migration and Invasion. *Ann. Ist. Super. Sanita* **2010**, *46*, 66–80.
17. Horwitz, R.; Webb, D. Cell Migration. *Curr. Biol.* **2003**, *13*, R756–R759.
18. Friedl, P.; Wolf, K. Tumor-Cell Invasion and Migration: Diversity and Escape Mechanisms. *Nat. Rev. Cancer* **2003**, *3*, 362–374.
19. Mercer, R. R.; Scabilloni, J.; Wang, L.; Kisin, E.; Murray, A. R.; Schwegler-Berry, D.; Shvedova, A. A.; Castranova, V. Alteration of Deposition Pattern and Pulmonary Response as a Result of Improved Dispersion of Aspirated Single Walled Carbon Nanotubes in a Mouse Model. *Am. J. Physiol. Lung Cell Mol. Physiol.* **2008**, *294*, L87–L97.
20. Shvedova, A. A.; Kisin, E. R.; Mercer, R.; Murray, A. R.; Johnson, V. J.; Poapovich, A. I.; Tyurina, Y. Y.; Gorelik, O.; Arepalli, S.; Schwegler-Berry, D.; *et al.* Unusual Inflammatory and Fibrogenic Pulmonary Responses to Single-Walled Carbon Nanotubes in Mice. *Am. J. Physiol. Lung Cell Mol. Physiol.* **2005**, *289*, L698–L708.
21. Stone, K. C.; Mercer, R. R.; Gehr, P.; Stockstill, B.; Crapo, J. D. Allometric Relationships of Cell Numbers and Size in the Mammalian Lung. *Am. J. Respir. Cell Mol. Biol.* **1992**, *6*, 235–243.
22. Takeuchi, T.; Nakajima, M.; Morimoto, K. A Human Cell System for Detecting Asbestos Cytogenotoxicity *in Vitro*. *Mutat. Res.* **1999**, *438*, 63–70.
23. Brown, J. S.; Zeman, K. L.; Bennet, W. D. Ultrafine Particle Deposition and Clearance in the Healthy and Obstructed Lung. *Am. J. Respir. Crit. Care Med.* **2002**, *166*, 1240–1247.
24. Shvedova, A. A.; Kisin, E.; Murray, A. R.; Johnson, V. J.; Gorelik, O.; Arepalli, S.; Hubbs, A. F.; Mercer, R. R.; Keohavong, P.; Sussman, N.; *et al.* Inhalation *vs.* Aspiration of Single-Walled Carbon Nanotubes in C57BL/6 Mice: Inflammation, Fibrosis, Oxidative Stress, and Mutagenesis. *Am. J. Physiol. Lung Cell Mol. Physiol.* **2008**, *295*, L552–L565.
25. Li, X.; Peng, Y.; Qu, X. Carbon Nanotubes Selective Destabilization of Duplex and Triplex DNA and Inducing B−A Transition in Solution. *Nucleic Acids Res.* **2006**, *34*, 3670–3676.
26. Sargent, L. M.; Hubbs, A. F.; Young, S. H.; Kashon, M. L.; Dinu, C. Z.; Salisbury, J. L.; Benkovic, S. A.; Lowry, D. T.; Murray, A. R.; Kisin, E. R.; *et al.* Single-Walled Carbon Nanotube-Induced Mitotic Disruption. *Mutat. Res.* **2012**, *745*, 28–37.
27. Xu, J.; Futakuchi, M.; Shimizu, H.; Alexander, D. B.; Yanagihara, K.; Fukamachi, K.; Suzui, M.; Kanno, J.; Hirose, A.; Ogata, A.; *et al.* Multi-walled Carbon Nanotubes Translocate into the Pleural Cavity and Induce Visceral Mesothelial Proliferation in Rats. *Cancer Sci.* **2012**, *103*, 2045–2050.
28. Heintz, N. H.; Janssen-Heininger, Y. M. W.; Mossman, B. T. Asbestos, Lung Cancers, and Mesotheliomas: From Molecular Approaches to Targeting Tumor Survival Pathways. *Am. J. Respir. Cell Mol. Biol.* **2010**, *42*, 133–139.
29. Sharma, C. S.; Sarkar, S.; Periyakaruppan, A.; Barr, J.; Wise, K.; Thomas, R.; Wilson, B. L.; Ramesn, G. T. Single-Walled Carbon Nanotubes Induces Oxidative Stress in Rat Lung Epithelial Cells. *J. Nanosci. Nanotechnol.* **2007**, *7*, 2466–2472.
30. Cho, S. Y.; Klemke, R. L. Extracellular-Regulated Kinase Activation and CAS/Crk Coupling Regulate Cell Migration and Suppress Apoptosis during Invasion of the Extracellular Matrix. *J. Cell Biol.* **2000**, *149*, 223–236.
31. Friedl, P.; Brucker, E. B. The Biology of Cell Locomotion with Three-Dimensional Extracellular Matrix. *Cell. Mol. Life Sci.* **2000**, *57*, 41–64.
32. Wang, L.; Luanpitpong, S.; Castranova, V.; Tse, W.; Lu, Y.; Pongrakhananon, V.; Rojanasakul, Y. Carbon Nanotubes Induce Malignant Transformation and Tumorigenesis of Human Lung Epithelial Cells. *Nano Lett.* **2011**, *11*, 2796–2803.
33. Lee, A. G.; Charles, A. V.; Norma, J. M.; Agnes, B. K. Growth Factor Responses and Protooncogene Expression of Murine Mesothelial Cell Lines Derived from Asbestos-Induced Mesotheliomas. *Toxicol. Pathol.* **1997**, *25*, 565–573.
34. Tamaoki, J.; Isono, K.; Takeyama, K.; Tagaya, E.; Nakata, J.; Nagai, A. Ultrafine Carbon Black Particles Stimulate Proliferation of Human Airway Epithelium *via* EGF Receptor-Mediated Signaling Pathway. *Am. J. Physiol. Lung Cell Mol. Physiol.* **2004**, *287*, L1127–L1133.
35. Lauffenburger, D. A.; Horwitz, A. F. Cell Migration: A Physically Integrated Molecular Process. *Cell* **1996**, *84*, 359–369.
36. Guo, N. L.; Wan, Y. W.; Denvir, J.; Porter, D. W.; Pacurari, M.; Wolfarth, M. G.; Castranova, V.; Qian, Y. Multi-walled Carbon Nanotube-Induced Gene Signatures in the Mouse Lung: Potential Predictive Value for Human Lung Cancer Risk and Prognosis. *J. Toxicol. Environ. Health A* **2012**, *75*, 1129–1153.
37. Park, E. J.; Roh, J.; Kim, S. N.; Kang, M. S.; Han, Y. A.; Kim, Y.; Hong, J. T.; Choi, K. A Single Intratracheal Instillation of Single-Walled Carbon Nanotubes Induced Early Lung Fibrosis and Subchronic Tissue Damage in Mice. *Arch. Toxicol.* **2011**, *85*, 1121–1131.
38. Passlick, B.; Sienel, W.; Seen-Hibler, R. Overexpression of Matrix Metalloproteinase 2 Predicts Unfavorable Outcome in Early-Stage Non-Small Cell Lung Cancer. *Clin. Cancer Res.* **2000**, *6*, 3944–3948.
39. Tan, R. J.; Fattman, C. L.; Niehouse, L. M.; Tobolewski, J. M.; Hanford, L. E.; Li, Q. L.; Monzon, F. A.; Parks, W. C.; Oury, T. D. Matrix Metalloproteinases Promote Inflammation and Fibrosis in Asbestos-Induced Lung Injury in Mice. *Am. J. Respir. Cell Mol. Biol.* **2006**, *35*, 289–297.
40. Stetler-Stevenson, W. G.; Aznavoorian, S.; Liotta, L. A. Tumor Cell Interactions with the Exstracellular Matrix during Invasion and Metastasis. *Annu. Rev. Cell Biol.* **1993**, *9*, 541–573.
41. Nagase, H.; Woessner, J. F., Jr. Matrix Metalloproteinase. *J. Biol. Chem.* **1999**, *274*, 21491–21494.
42. Birkedal-Hansen, H.; Moore, W. G.; Bodden, M. K. Matrix Metalloproteinases: A Review. *Crit. Rev. Oral Biol. Med.* **1993**, *4*, 197–250.
43. Coussens, L. M.; Werb, Z. Matrix Metalloproteinases and the Development of Cancer. *Chem. Biol.* **1996**, *3*, 895–904.
44. Wang, A.; Zhang, B.; Huang, H.; Zhang, L.; Zeng, D.; Tao, Q.; Wang, J.; Pan, C. Suppression of Local Invasion of Ameloblastoma by Inhibition of Matrix Metalloproteinase-2 *in Vitro*. *BMC Cancer* **2008**, *8*, 182.
45. Shen, Y. G.; Xu, Y. J.; Shi, Z. L.; Han, H. L.; Sun, D. Q.; Zhang, X. Effects of RNAi-Mediated Matrix Metalloproteinase-2 Gene Silencing on the Invasiveness and Adhesion of Esophageal Carcinoma Cells, KYSE150. *Dig. Dis. Sci.* **2012**, *57*, 32–37.
46. Masson, V.; Ballina, L. R.; Munaut, C.; Wielockx, B.; Jost, M.; Maillard, C.; Blacher, S.; Bajou, K.; Itoh, T.; Itohara, S.; *et al.*

Contribution of Host MMP-2 and MMP-9 To Promote Tumor Vascularization and Invasion of Malignant Keratinocytes. *FASEB* **2004**, *19*, 234–236.
47. Tokuraku, M.; Sato, H.; Murakami, S.; Okada, Y.; Watanabe, Y.; Seiki, M. Activation of the Precursor of Gelatinase A/72 kDa Type IV Collagenase/MMP-2 in Lung Carcinomas Correlates with the Expression of Membrane Type Matrix Netalloproteinase (MT-MMP) and with Lymph Node Metastasis. *Int. J. Cancer* **1995**, *64*, 355–359.
48. Suzuki, M.; Kobayashi, H.; Kanayama, N.; Saga, Y.; Suzuki, M.; Lin, C. Y.; Dickson, R. B.; Terao, T. Inhibition of Tumor Invasion by Genomic Down-Regulation of Matriptase through Suppression of Activation of Receptor-Bound Pro-Urokinase. *J. Biol. Chem.* **2004**, *279*, 14899–14908.
49. Li, H.; Daculsi, R.; Bareille, R.; Bourget, C.; Amedee, J. uPA and MMP-2 Were Involved in Self-Assembled Network Formation in a Two Dimensional Co-culture Model of Bone Marrow Stromal Cells and Endothelial Cells. *J. Cell. Biochem.* **2013**, *114*, 650–657.
50. Mi, Z.; Guo, H.; Wai, P. Y.; Gao, C.; Kuo, P. C. Integrin-Linked Kinase Regulates Osteopontin-Dependent MMP-2 and uPA Expression To Convey Metastatic Function in Murine Mammary Epithelial Cancer Cells. *Carcinogenesis* **2006**, *27*, 1134–1145.
51. Xie, T. X.; Huang, F. J.; Aldape, K. D. Activation of Stat3 in Human Melanoma Promotes Brain Metastasis. *Cancer Res.* **2006**, *66*, 3188–3196.
52. Xie, T. X.; Wei, D.; Liu, M.; Gao, A. C.; Osman, F. A.; Sawaya, R.; Huang, S. Stat3 Activation Regulates the Expression of Matrix Metalloproteinase-2 and Tumor Invasion and Metastasis. *Oncogene* **2004**, *23*, 3550–3560.
53. Yu, C. L.; Meyer, D. J.; Campbell, G. S.; Lamer, A. C.; Carter-Su, C.; Schwartz, J.; Jove, R. Enhanced DNA-Binding Activity of a Stat3-Related Protein in Cells Transformed by the Src Oncoprotein. *Science* **1995**, *269*, 81–83.
54. Jin, E. J.; Park, K. S.; Bang, O. S.; Kang, S. S. Akt Signaling Regulates Actin Organization *via* Modulation of MMP-2 Activity during Chondrogenesis of Chick Wing Limb Bud Mesenchymal Cells. *J. Cell. Biochem.* **2007**, *102*, 252–261.
55. Park, B. K.; Zeng, X.; Glazer, R. I. Akt1 Induces Extracellular Matrix Invasion and Matrix Metalloproteinase-2 Activity in Mouse Mammary Epithelial Cells. *Cancer Res.* **2001**, *61*, 7647–7653.
56. Hu, J.; Chen, C.; Su, Y.; Du, J.; Qian, X.; Jin, Y. Vascular Endothelial Growth Factor Promotes the Expression of Cyclooxygenase 2 and Matrix Metalloproteinases in Lewis Lung Carcinoma Cells. *Exp. Ther. Med.* **2012**, *4*, 1045–1050.
57. Murphy, G.; Gavrilovic, J. Proteolysis and Cell Migration: Creating a Path? *Curr. Opin. Cell Biol.* **1999**, *11*, 614–621.
58. Kohn, E. C.; Liotta, L. A. Molecular Insights into Cancer Invasion: Strategies for Prevention and Intervention. *Cancer Res.* **1995**, *55*, 1856–1862.
59. Grigioni, W. F.; D'Errico, A.; Fortunato, C. Prognosis of Gastric Carcinoma Revealed by Interactions between Tumor Cells and Basement Membrane. *Mol. Pathol.* **1994**, *7*, 220–225.
60. Sáinz-Jaspeado, M.; Lagares-Tena, L.; Lasheras, J. Caveolin-1 Modulates the Ability of Ewing's Sarcoma To Metastasize. *Cancer Res.* **2010**, *8*, 1489–1500.
61. Tanaka, S.; Choe, N.; Iwagaki, A.; Hemenway, D. R.; Kagan, E. Asbestos Exposure Induces MCP-1 Secretion by Pleural Mesothelial Cells. *Exp. Lung Res.* **2000**, *26*, 241–255.
62. Shvedova, A. A.; Fabisiak, J. P.; Kisin, E. R.; Murray, A. R.; Roberts, J. R.; Tyurina, Y. Y.; Antonini, J. M.; Feng, W. H.; Kommineni, C.; Reynolds, J.; *et al.* Sequential Exposure to Carbon Nanotubes and Bacteria Enhances Pulmonary Inflammation and Infectivity. *Am. J. Respir. Cell Mol. Biol.* **2008**, *38*, 579–590.
63. Ahmed, S.; Pakozdi, A.; Koch, A. E. Regulation of Interleukin-1β-Induced Chemokine Production and Matrix Metalloproteinase-2 Activation by Epigallocatechin-3-Gallate in Rheumatoid Arthritis Synovial Fibroblasts. *Arthritis Rheum.* **2006**, *54*, 2393–2401.
64. Pan, J.; Chang, Q.; Wang, X.; Son, Y.; Zhang, Z.; Chen, G.; Luo, J.; Bi, Y.; Chen, F.; Shi, X. Reactive Oxygen Species-Activated Akt/ASK1/p38 Signaling Pathway in Nickel Compound-Induced Apoptosis in BEAS 2B Cells. *Chem. Res. Toxicol.* **2010**, *23*, 568–577.
65. Habibzadegah-Tari, P.; Byer, K. G.; Khan, S. R. Reactive Oxygen Species Mediated Calcium Oxalate Crystal-Induced Expression of MCP-1 in HK-2 Cells. *Urol. Res.* **2006**, *34*, 26–36.
66. Wang, L.; Castranova, V.; Mishra, A.; Chen, B.; Mercer, R. R.; Schwegler-Berry, D.; Rojanasakul, Y. Dispersion of Single-Walled Carbon Nanotubes by a Natural Lung Surfactant for Pulmonary *In Vitro* and *In Vivo* Toxicity Studies. *Part. Fibre Toxicol.* **2010**, *7*, 31–41.
67. Wang, L.; Stueckle, T. A.; Mishra, A.; Derk, R.; Meighan, T.; Castranova, V.; Rojanasakul, Y. Neoplastic Transformation Effect of Single-Walled and Multi-Walled Carbon Nanotubes *vs*. Asbestos on Human Lung Small Airway Epithelial Cells. *Nanotoxicology* **2013**, 10.3109/17435390.2013.801089.
68. Mishra, A.; Rojanasakul, Y.; Chen, B. T.; Castranova, V.; Mercer, R. R.; Wang, L. Assessment of Pulmonary Fibrogenic Potential of Multiwalled Carbon Nanotubes in Human Lung Cells. *J. Nanomater.* **2012**, 10.1155/2012/930931.
69. Porter, D. W.; Hubbs, A. F.; Mercer, R. R.; Wu, N.; Wolfarth, M. G.; Sriram, K.; Leonard, S.; Battelli, L.; Schwegler-Berry, D.; Friend, S.; *et al.* Mouse Pulmonary Dose- and Time Course-Responses Induced by Exposure to Multi-walled Carbon Nanotubes. *Toxicology* **2010**, *269*, 136–147.
70. Kesanakurti, D.; Chetty, C.; Dinh, D. H.; Gujrati, M.; Rao, J. S. Role of MMP-2 in the Regulation of IL-6/Stat3 Survival Signaling *via* Interaction with $\alpha 5\beta 1$ Integrin in Glioma. *Oncogene* **2013**, *32*, 327–340.
71. Stueckle, T. A.; Lu, Y.; Davis, M. E.; Wang, L.; Jiang, B. H.; Holaskova, I.; Schafer, R.; Barnett, J. B.; Rojanasakul, Y. Chronic Occupational Exposure to Arsenic Induces Carcinogenic Gene Signaling Networks and Neoplastic Transformation in Human Lung Epithelial Cells. *Toxicol. Appl. Pharmacol.* **2012**, *261*, 204–216.